

Reproducible Echocardiography in Juvenile Sheep and its Application in the Evaluation of a Pulmonary Valve Homograft Implant

TAO HONG, MD,^{1,3} MARY S. MAISH, MD,^{1,3} JENNIFER COHEN,¹ PAUL FITZPATRICK,¹ ARTHUR A. BERT, MD,³ JAMES S. HARPER, III, VMD,² DONGYU FANG, MD,³ DIANE HOFFMAN-KIM, PHD,^{1,3} AND RICHARD A. HOPKINS, MD^{1,3}

Abstract | Increased use of the ovine animal model in cardiovascular surgical research has created a salient need for standardized echocardiography techniques. To demonstrate a reproducible image in this species and confirm the validity of echocardiography as a diagnostic tool, we implanted 10 sheep with a pulmonary valve homograft and monitored them through weekly echocardiographic examinations until 20 weeks after implantation. We obtained good images from the left cranial and the left caudal transducer windows without needing to sedate the animals. Sedated sheep yielded adequate views from the right apical window. Echocardiographic data on the implanted homografts (including functional capacity, presence of calcification, and hemodynamic information and measurements), completely agreed with the results of the post-explantation examinations.

Echocardiography is a proven and useful diagnostic tool for evaluating the structural, functional, and hemodynamic status of the cardiovascular system. This form of ultrasonic imaging is prevalent in human medicine and is becoming increasingly popular in veterinary practices. Described among the most rewarding of the veterinary tests available (1), this diagnostic tool is non-invasive, innocuous, and portable. In addition, most veterinary echocardiographic examinations are conducted without sedating the animal. These factors, combined with the wide range of clinical and research applications, have made veterinary echocardiography a rapidly growing field.

The juvenile sheep is a model for testing human chronic cardiac implants. There is an emerging need for a documented echocardiographic protocol for the sheep species. The purposes of our study were to develop a technique for generating reproducible echocardiographic images in sheep, to assess whether sedation is necessary for an effective ovine echocardiographic examination, to define the windows and angles of view that grant the best echocardiographic images in the sheep model and to use this information to evaluate a pulmonary valve homograft implant through a 20-week period, and to compare the echocardiographic findings to the post-explantation data.

Materials and Methods

Animals and husbandry. From Parson's Farm (North Hampton, MA), we obtained one male and nine female domestic sheep (*Ovis aries*) of a Rambouillet, Dorset, Hampshire, and Suffolk breed mix that were 20 to 40 weeks old and weighed 35 to 44 (mean, 40.1 ± 1.7) kg at the time of surgery. Upon arrival at the Brown University Animal Care Facility, all animals were evaluated by the veterinarian staff and certified to be pathogen-free. The sheep were kept on standard wood shavings in pens of at least 30 square feet, with two animals in each pen. All sheep received a ration of alfalfa hay twice daily and water ad libitum. Although sheep were sheared prior to arrival, room temperatures were maintained at 22 to 25°C. Animals were acclimated for at least 5 days prior to implantation surgery. This study was approved by the IACUC and was performed in accordance with the *Guide for Care and Use of Laboratory Animals*.

Surgical protocol. *Anesthesia* For preoperative sedation, the animals received acetylpromazine (0.2 mg/kg intramuscularly; Fort Dodge Animal Health, Fort Dodge, IA) 20 min before transportation to the operating room; upon the sheep's arrival, anesthesia was induced by using propofol (4 to 6 mg/kg IV; Zeneca Pharmaceuticals, Caponago, Italy) and maintained by using 1–1.3 mg/kg MAC isoflurane (Abbott Labs, Abbott Park, IL). Fentanyl (5 µg/kg intravenously; Elkins-Sian, Cherry Hill, NJ) was given just prior to thoracotomy and supplemented at 1 µg/kg during cardiac bypass. Doses of propofol (1.5 mg/kg) every 5 min supplemented anesthesia during cardiac bypass. Prior to closure of the thoracotomy, we infused 30 mL 0.5% bupivacaine (Astra, Westborough, MA) around the wound and close to the dorsal nerve roots. The sheep received their first doses of ketorolac (30 mg; Abbott Labs) and buprenorphine (0.3 mg/kg; Elkins-Sian) for postoperative analgesia during closure of the thoracotomy. Systolic blood pressure was maintained above 80 mm Hg before and after cardiac bypass and above 50 mm Hg during cardiac bypass. Central venous pressure was maintained at 6 to 12 mm Hg throughout the surgery.

Implantation procedure We secured the anesthetized sheep to the operating table in left lateral recumbency and sheared, scrubbed, and draped the surgical area. A left thoracotomy was performed, and the chest was entered through the fifth intercostal space. We then created a right-heart bypass circuit by inserting heparin-bonded cannulae into the distal pulmonary artery and the right atrium. We connected the cannulae to a roller pump head in a circuit that contained an oxygenator (to maintain oxygen saturation > 97%) and a thermostat (to maintain normothermia). The pulmonary artery was mobilized, and we applied a vascular clamp just distal to the bifurcation and proximal to the insertion of the arterial cannula. The native pulmonary leaflets were excised while the right ventricle was kept empty by the right-heart bypass circuit. The cryopreserved sheep pulmonary homograft (obtained through a gift from Lifenet, Norfolk, VA) was sutured as an interposition graft. The proximal and distal end-to-end anastomoses were accomplished by using a running 4-0 prolene suture, after which the bypass shunt was occluded. The vascular clamps then were removed, a chest tube was inserted, and the chest was closed. The animal was extubated as soon as it regained adequate ventilation and consciousness. The chest tube was removed within 6 h after

Collis Cardiovascular Research Laboratory, Rhode Island Hospital, Department of Animal Care, and Department of Surgery (Cardiac Surgery), Brown University School of Medicine Providence, RI

completion of surgery.

For 3 days after implantation, intramuscular amikacin (10 mg/kg; Phoenix Scientific Inc., Hailsham, East Sussex, UK), amoxicillin (5 to 10 mg/kg; Pfizer Animal Health, Exton, PA), buprenorphine (0.3 mg/kg), and ketoralac (15 mg) were administered twice daily. After day 3, buprenorphine was discontinued while dosages of other medications remained the same. After day 5, ketoralac was discontinued, and the amikacin and amoxicillin doses were reduced to once daily. Following the recommendation of the Chief of Veterinary Medicine at Brown University, we maintained these antibiotics at this dosage throughout the 20-week chronic phase of the investigation.

Explantation procedure. At the end of the 20-week chronic implantation phase, the homografts were explanted, and the animals were euthanized by using 360 mg/kg intravenous pentobarbital (Sparhawk Vet Labs, Lenexa, KS), which we administered to the animal while it was anesthetized under 2% expired isoflurane. We examined the explanted homograft to determine whether the echocardiographic data was consistent with the pathology of the explanted tissue. A water test was performed to check the homograft and valve for leaks and potential regurgitation, and we used a ruler to measure the diameter of the homograft when it was under zero pressure.

Echocardiographic examination and evaluation. Each sheep underwent echocardiographic examination both before and after the implantation surgery. These pre-operative and post-operative examinations were conducted both with and without sedation on all animals studied. All animals received exams pre-operatively (no sedation), just prior to implantation (under sedation), weekly post-operatively (weeks 2 through 20; no sedation), and just prior to explantation (under sedation).

Echocardiograph procedure. To rotate the heart to the optimal position in the chest, the sheep was placed in left lateral recumbency with the left foreleg elevated and the head and legs immobilized. We used the HP Sonos 1000 (Hewlett-Packard, Andover, MA) echocardiography system and a 2.5- or 3.5-MHz transducer to perform the evaluation. All images were obtained by a single operator and were recorded on video (Panasonic VHS, Matsushita Electric, Osaka, Japan) for later analysis.

The exam began with a two-dimensional study using three different transducer locations: the left cranial, left caudal, and right apical windows. In the left cranial window, we placed the transducer along the left side of the sternum at approximately the third intercostal space and oriented the transducer toward the left hindleg of the sheep to obtain a short-axis picture of the base of the heart. In the left caudal window, we placed the transducer along the left side of the sternum at approximately the fifth intercostal space. We then rotated the transducer 90° clockwise to obtain a view of the long axis of the heart. By changing the angle of the transducer, we could see the short axis of the left ventricle through this window. Views through the right apical window were obtained by placing the transducer immediately to the right of the sternum in approximately the sixth intercostal space. By rotating the transducer, we obtained two-, four-, and five-chambered views of the heart. Thus six views were obtained via the three windows.

To achieve reproducible images from the same tomographic planes, we established intracardiac reference points. We obtained the long axis views from the right and left sides by orienting the scan plane parallel to the longitudinal cardiac axis. Conversely, the short-axis pictures were obtained by orienting the scan plane perpendicular to that of the long axis. As in human echocardiography, the orientation of the picture viewed on the monitor was independent of the placement of the transducer on the animal. Regardless of the site of transducer placement in the chest, the images consistently showed the apex of the heart on the left and the base of the heart (atria, great vessels) on the

right. In addition, the four- and five-chamber views uniformly were oriented with the apex at the top of the screen, the mitral valve on the right, and tricuspid valve on the left. Echocardiographic images were considered to be "good" if all structures in a given window could be seen clearly and measured. "Adequate" images were defined as those in which all structures in a given window were seen clearly but could not be measured. Images in which all structures in a given window were not seen clearly were deemed "inadequate."

We used the left cranial window to measure the diameter of the distal anastomoses. We analyzed each recorded session frame-by-frame and noted the maximum diameter. The residue of the native pulmonary leaflets and the implanted homograft were visible from this window. In addition, this view enabled us to assess valvular thickening and calcification.

We used color-flow Doppler echocardiography to demonstrate valve regurgitation. The size of the regurgitation jet of the implanted homograft valve was semiquantified by mapping the area of turbulent diastolic blood flow within the right ventricular outflow tract (RVOT). The homograft pulmonary regurgitation was considered to be slight (1+) if the jet occurred only immediately behind the valve, mild (2+) if the regurgitation jet was limited to the RVOT, moderate (3+) if the regurgitation jet was seen in the right ventricle, and severe (4+) if the regurgitation jet reached the tricuspid valve. We measured the peak instantaneous pressure gradient between the homograft pulmonary valve and pulmonary artery by placing the sensor in the distal homograft in the left cranial window view. To optimize this process, the Doppler beam was always parallel to the pulmonary artery.

Statistical analysis. Results are reported as the mean \pm one standard deviation. We used Student's *t* test to determine whether the size of the homograft found by using a ruler prior to implantation varied from that obtained by using echocardiography 2 weeks after implantation. We also used Student's *t* test to determine if there was a significant difference between homograft size prior to implantation and homograft size measured with echocardiography at 10 weeks, 20 weeks, and after implantation. In addition, we used Student's *t* test to determine the statistical significance of differences between the size of the homograft measured by using a ruler after explantation and that found by using echocardiography in sedated and unsedated animals at 20 weeks after implantation. For all analyses, the level of significance was set at 0.05. To document reproducibility, a Pearson's concordance correlation coefficient was calculated.

Results

All 10 sheep survived the implantation of a right ventricular outflow homograft valve and the 20-week postoperative evaluation phase. Although we used both 2.5- and 3.5-MHz transducers during the first few examinations, we abandoned use of the 3.5-MHz transducer because of its lack of penetration.

We obtained what we defined as "good" images of the heart through the left cranial and left caudal windows in 85% (N = 160) of all the images from unsedated sheep. From the right apical view, "good" images were obtained in only 15% (N = 120) of the examinations conducted on unsedated animals. For examinations of the left cranial and caudal windows on sedated animals, 100% (N = 16) of the images obtained were "good." Examinations of the right apical window in sedated sheep returned "good" images 50% of the time, with adequate images obtained in another 10% of examinations. Image quality was based on the best images obtained during each examination period.

Results of pre-implantation echocardiography. The left atrium (LA), right atrium (RA), tricuspid valve (TV), right ventricle (RV), RVOT, pulmonary valve (PV), aortic valve (AV) and ascending aorta all were visible through the left cranial window

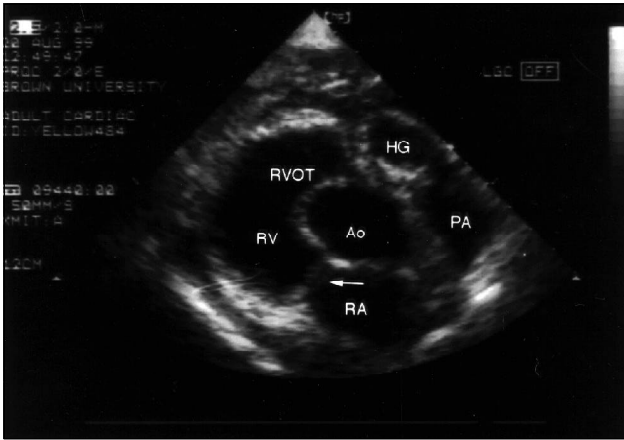


FIG. 1. The left cranial view shows the base of the heart in systole. RA, right atrium; RV, right ventricle; RVOT, right ventricular outflow tract; HG, homograft; PA, pulmonary artery; Ao, Aorta; Arrow, tricuspid valve in close position.

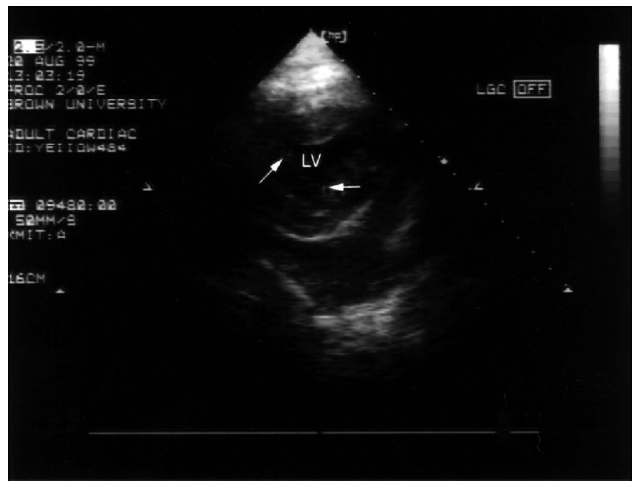


FIG. 4. Left caudal window, short axis of left ventricle—the papillary muscle level. LV, left ventricle; Arrow, papillary muscle.

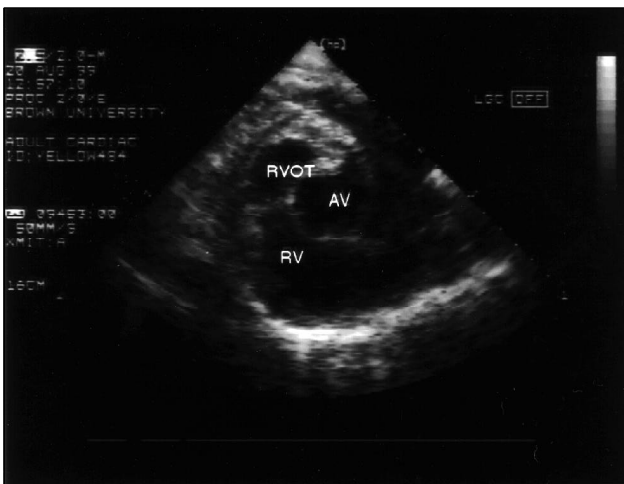


FIG. 2. The left cranial view shows the aortic valve. AV, aortic valve; RV, right ventricle; RVOT, right ventricular outflow tract.

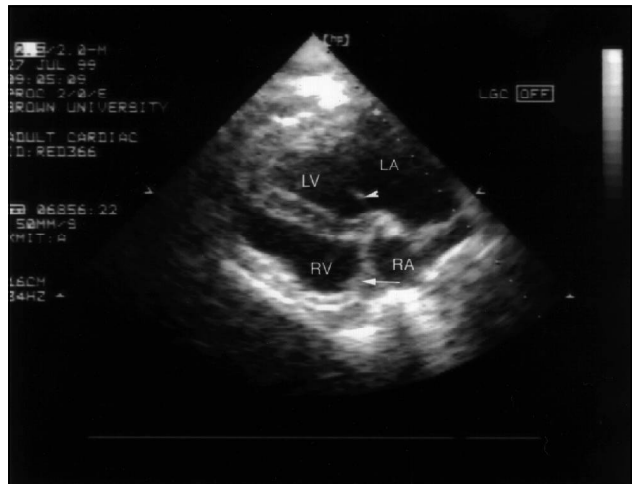


FIG. 5. The apical four chambered view in diastole. RA, right atrium; RV, right ventricle; LA, left ventricle; LV, left ventricle; Arrow, tricuspid valve; Arrow head, mitral valve.



FIG. 3. The left caudal window shows the four chambered view in systole. RA, right atrium; RV, right ventricle; LA, left atrium; LV, left ventricle; Arrow, tricuspid valve; Arrow head, mitral valve.

(Figure 1). Rotation or angulation of the transducer easily enabled us to trace the pulmonary artery (PA) to its bifurcation. The AV was seen beneath the PA. Rotating the transducer yielded a clear image of the aortic leaflets. The three leaflets of the aor-

tic valves (right, left, and non-coronary) could be identified during both diastole and systole (Figure 2).

The long-axis view through the left caudal window yielded a four-chambered image of the heart (Figure 3). Orientation of the heart in these images was such that the apex consistently occurred at the left of the screen, and the atria consistently were on the right. Color-flow Doppler failed to identify any aortic or mitral regurgitation in any of the 10 sheep.

We obtained a short-axis view of the heart through the left caudal window at three different levels. At the level of the mitral valve (MV), the anterior and posterior leaflets of this valve were visible. The level of papillary muscles as they encroached on the cavity of the left ventricle was identified easily by the outline of the papillary muscles as they encroached on the cavity of the left ventricle (Figure 4). The echoes of the origins of the chordae tendineae appeared on the screen as high-density points. The apical level afforded a view of the cardiac apex, but neither the mitral valve nor the papillary muscles were visible at this level.

In the right apical window, rotation of the transducer returned two-, four-, and five-chambered views of the heart. From the right apical two-chambered view (along the long axis of the left ventricle), the left ventricle (LV), LA, and MV could be visualized; the aorta was not seen from this view. We obtained the right apical four-chambered view by rotating the transducer counter-clockwise from its position for the right apical two-chambered view (Figure 5). Similar to the four-chambered apical image in



FIG. 6. The apical five chambered view. Ao, Aorta; LA, left atrium; LV, left ventricle; RA, right atrium; RV, right ventricle; Arrow, aortic valve; Arrow head, mitral valve.

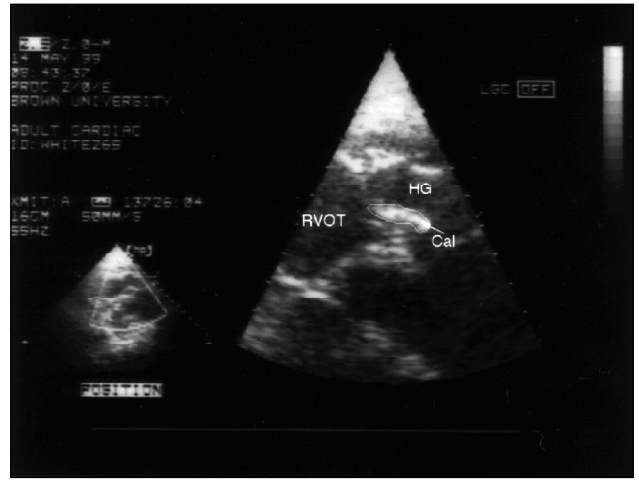


FIG. 8. The calcification of the homograft wall. Arrow, calcification plaque; HG, homograft; RVOT, right ventricle outflow tract.

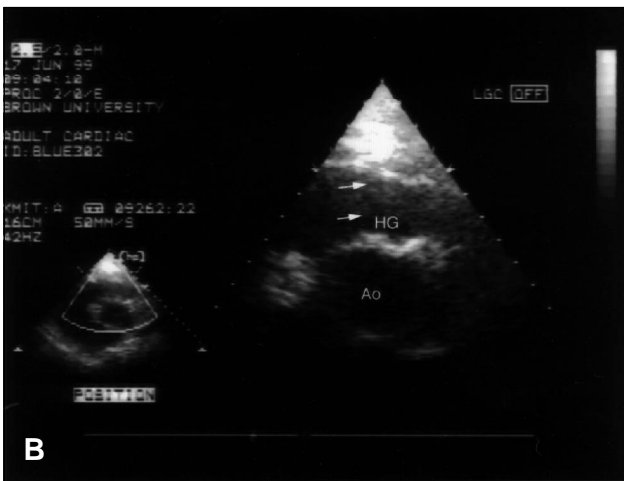
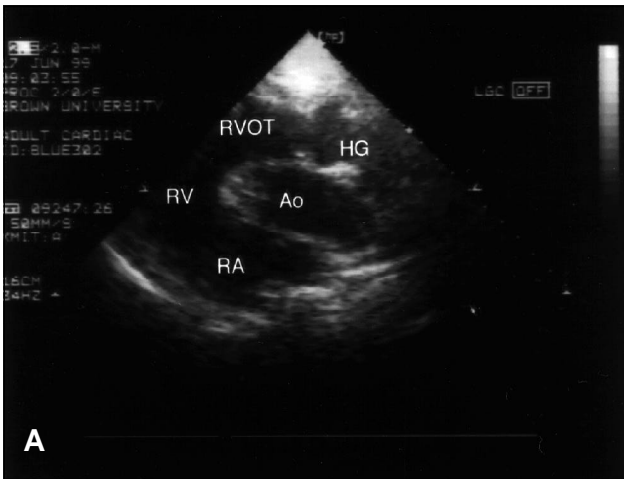


FIG. 7. Echocardiography of the implant homograft. (A) Implant homograft. RA, right atrium; RV, right ventricle; RVOT, right ventricular outflow tract; HG, homograft; Ao, Aorta. (B) Amplified view of the homograft. HG, homograft; Arrow, homograft leaflet.

human echocardiography, this view of the sheep heart yielded images of the four chambers of the heart, the MV, and the TV. Angulation of the transducer produced the right apical five-chambered view, which imaged the four chambers of the heart and the MV, TV, aorta, and AV (Figure 6).

Results of post-implantation echocardiography. We used the left cranial window for the weekly examinations of the implanted cryopreserved pulmonary homograft implant. Angling the transducer enabled visualization of the length of the implanted homograft and the path of the PA to the bifurcation (Figure 7). The homograft leaflets, readily seen during diastole, appeared thicker than the remnants of the native pulmonary leaflets. The wall of the homograft in two of our sheep contained areas of increased density, which are often indicative of (but not diagnostic of) calcification (Figure 8). Two of the implanted homograft valves showed I+ regurgitation.

We used spectral Doppler flow echocardiography to measure pressure gradients between the PA and the distal end of the anastomoses. Because a normal range for these pressure gradients has not been established, comparison of our findings was impossible.

Using the matched pairs t-test revealed statistically significant growth of the homograft diameter between implantation and week 10 ($p = .003$), implantation and week 20 ($p = 0.005$), week 10 and explantation ($p = 0.01$), and implantation and explantation ($p = 0.001$; Table 1). The correlation between the size of the homograft at implantation and that on the week 2 echocardiogram was $r = 0.811$; this value was $r = 0.922$ for the size of the homograft at explantation vs that on the week 20 echocardiogram. Therefore the size of the homograft measured from the echocardiogram correlates well with that obtained directly by using a ruler.

The echocardiograms of two sheep revealed areas of increased density (indicative of calcification) in the homograft wall. Visual examination upon explantation confirmed the presence of calcification in both animals. A water test on the explanted homograft showed that the leaflets were competent in the remaining eight animals. The leaflets of all 10 explanted homografts appeared thicker than those of the native PV. The echocardiographic measurements of the distal anastomosis are shown in Table 1.

Discussion

Previous use of echocardiography in small animal medicine has revealed the presence of many congenital and acquired cardiac defects in cats and dogs. Mitral regurgitation as well as dilated, restrictive, and hypertrophic cardiomyopathies in these animals have all been documented (2, 3) largely due to the role of echocardiography as a veterinary diagnostic tool. Large-animal echocardiographic studies were pioneered by Pipers in the late 1970s. Reproducible echocardiograph images in horses (4),

Table 1. Comparison between diameters (in cm) of the homograft as measured directly by using a ruler prior to implantation and after explantation and those deduced from the echocardiographic images of the distal anastomoses obtained at various times after implantation

Animal no.	Prior to implantation	Week 2	Week 10	Week 20	After explantation
1	1.8	1.78	1.91	2.2	2.3
2	1.6	1.71	1.72	1.8	2.1
3	1.7	1.79	1.90	2.1	2.3
4	1.5	1.59	1.77	1.8	1.9
5	1.5	1.64	1.73	1.8	1.9
6	1.5	1.60	1.83	1.8	1.8
7	1.5	1.51	1.74	1.8	1.8
8	1.5	1.52	1.62	1.7	1.8
9	1.6	1.62	1.60	1.6	1.6
10	1.7	1.64	1.65	1.7	1.7

cows (5) and swine (6) all have been documented. Since then, extensive studies have been conducted examining standardized imaging for both the equine (7, 8) and bovine (9) species. Large-animal investigations analogous to the canine and feline studies have revealed multiple cases of severe equine mitral regurgitation (4), bovine patent ductus arteriosus (9), anomalies of the tricuspid valve in goats (10), and many other cardiac defects.

Despite the growing interest surrounding both bovine and equine echocardiography, the application to sheep models is relatively young. Like the pig, a well-known model for numerous research endeavors (6), the sheep has been used increasingly in cardiovascular research. Ovine models have been used to study a variety of cardiac parameters, including basic physiology (11–14), conduction pathways (15), fetal circulation (16), chronic cardiac disease (17), and the valvular apparatus (18–20). This expanding use of the ovine animal model represents an academically compelling and economically beneficial reason for further investigations in sheep echocardiography. Currently in human medicine or studies conducted on other species than sheep, any cardiac implant would be monitored weekly through echocardiographic examinations. Without this tool, studies using sheep are limited to post-explantation evaluations of the implant and are further hindered by the inability to observe the implant functioning in the animal model. These evaluative holes in the cardiac implant research process accentuate the need for documented data applying the echocardiographic imaging technique to the sheep species.

Although the body of research using the ovine model to assess cardiac pathophysiology is growing, little of it focuses on the valvular apparatus. Several studies have focused in defining normal (14) and abnormal (11, 12, 15) cardiac physiology by using sheep. As in our study, valvular thickening and calcification has been documented by using echocardiography and confirmed upon necropsy (18). The application of echocardiography to evaluate the valvular apparatus in sheep has been limited thus far to assessment of the physiology (20, 21) of the valve rather than to assess changes in the anatomy of the valve. Our study demonstrates that accurate measurements of the valve can be obtained in a sheep model by using two-dimensional echocardiography (2DE). Furthermore, these measurements correlate with explantation data and have proven to be reproducible.

A standardized echocardiographic image is attainable in the sheep model. Throughout the 20-week chronic period of this study, we visualized long and short axis views of the sheep heart from three different anatomical windows. We found the position of left lateral recumbency most suitable for both the left cranial and left caudal windows. From this position, the transducer was easily placed in the upper left chest area. The gravitational force in this position moves the heart to the right of the thoracic cavity. Consequently, the transducer is placed on

the right side of the lower sternum to achieve the view from the apical window. Because one of the leading disadvantages of echocardiography resides in difficulties encountered when applying diagnostic ultrasound to air-filled structures (1), avoiding the lung is important when conducting examinations. In each of these two windows, we could avoid obstruction from the lung by placing the transducer in the appropriate intercostal space and having the animal in left lateral recumbency. Effective evasation of the lungs is achieved because surgical adhesions adhere the heart to the chest wall. This effect prevents the lung from interfering with the ultrasound waves and allows for better resolution. For this reason, images in the presurgical sheep were more difficult to obtain. Although the left cranial window was still easily viewed in normal sheep (those that had not yet been implanted), both the left caudal and the apical views were markedly more challenging in sedated as well as unsedated pre-operative animals.

Sedation was unnecessary to achieve clear images from both the left caudal and the left cranial windows in implanted sheep. We obtained consistent pictures from all postoperative sheep by using these windows during the unsedated weekly examinations. Although the view from the right apical window was difficult to obtain without sedation, it was quite feasible while the animal was sedated and breathing on a ventilator. In addition to the increased maneuverability of the animal under sedation, another potential explanation for this increased ease of imaging may lie in the ability to control the tidal volume of the sheep on the ventilator. Increased muscle relaxation of the sedated animal is likely to have aided the examination as well. Despite difficulty in obtaining useful images from the right apical window during the unsedated weekly examinations, we were able to obtain all needed information about the cardiac chambers, the valves, and the myocardium by using the left caudal and left cranial windows.

The information afforded by the echocardiograph enabled a detailed evaluation of cardiac anatomy and physiology in the sheep examined. Thomas et al. (13) recommended standardized imaging planes and display conventions using three different windows of echocardiography in cats and dogs. Although we adopted these standardized techniques in our examinations, our study (unlike Thomas's) used image display orientations that were similar to those for human cardiac images, with the base or cranial aspect of the heart displayed to the examiner's right on the video monitor. In our sheep, the left cranial view afforded images of the short-axis view of the right atrium and ventricle, TV, PA, PV, and AV. From the left caudal window, the four-chamber (RA, RV, LA, LV) view of the heart, MV, TV, and the three levels of the left ventricle were seen. The right apical window afforded visualization of the two-chambered view (LA, LV), four-chambered view, and five-chambered view (RA, RV, LA, LV, aorta).

The echocardiographic images described above were reproducible in all the sheep examined. Despite this consistency in imaging, we observed interindividual differences in the location of the transducer windows. Long et al. (7) described considerable variation in transducer placement between horses, similar to our findings in sheep. Because of this variation, we defined each window by transducer placement and by using intracardiac landmarks in order to achieve standardized images from one animal to another. Defining cardiac images in this way should facilitate teaching, communication of diagnostic results, and translation of animal studies to the medical literature.

Voros et al. (8) studied 15 horses to validate the cardiac anatomy as seen in 2DE and to determine the accuracy of intracardiac measurements. They found that the in vivo 2DE images corresponded well with those from in vitro 2DE recordings and the data from anatomical sections. Reproducible imaging of each tomographic plane was possible on the post mortem hearts by using intracardiac reference points. Comparison of parameters measured during in vitro 2DE and autopsy demonstrated significant correlation between all 2DE and necropsy data.

We obtained reproducible echocardiographic images from unsedated juvenile sheep prior to and after implantation of right ventricular homograft valves. We describe a technique for generating high-quality reproducible echocardiographic images of the sheep heart. We believe our technique is a valuable tool for evaluating the fate of biological cardiac implants in vivo.

Acknowledgments

We thank Gary Stearns and Eric Gustafson for their excellent technical assistance. This project was supported by grants from Charles and Ellen Collis, the Children's Heart Foundation, and Medtronic, Inc.

References

1. **Moses, B. L., and J. V. Ross.** 1987. M-mode echocardiographic values in sheep. *Am. J. Vet. Res.* **48**:1313–1317.
2. **Birchard S. J., W. A. Ware, T. W. Fossum, et al.** 1986. Chylothorax associated with congestive cardiomyopathy in a cat. *J. Am. Vet. Med. Assoc.* **189**:1462–1464.
3. **Bright, J. M., and M. M. McEntee.** 1995. Isolated right ventricular cardiomyopathy in a dog. *J. Am. Vet. Med. Assoc.* **207**:64–66.
4. **Pipers, F. S., and R. L. Hamlin.** 1977. Echocardiography in the horse. *J. Am. Vet. Med. Assoc.* **170**:815–819.
5. **Pipers, F. S., V. Reef, R. L. Hamlin, et al.** 1979. Echocardiography in the bovine animal. *Bovine Pract.* **13**:114–118.
6. **Pipers, F. S., W. W. Muir, and R. L. Hamlin.** 1978. Echocardiography in swine. *Am. J. Vet. Res.* **39**:707–710.
7. **Long, K. J., J. D. Bonagura, and P. G. Darke.** 1992. Standardized imaging technique for guided M-mode and Doppler echocardiography in the horse. *Equine Vet. J.* **24**:226–235.
8. **Voros, K., J. R. Holmes, and C. Gibbs.** 1990. Anatomical validation of two-dimensional echocardiography in the horse. *Equine Vet. J.* **22**:392–397.
9. **Amory H., S. Jakovljevic, and P. Lekeux.** 1991. Quantitative M mode and two-dimensional echocardiography in calves. *Vet. Rec.* **12**:25–30

10. **Gardner, S.Y., V. B. Reef, J. Palmer, et al.** 1992. Echocardiographic diagnosis of an anomaly of the tricuspid valve in a male pygmy goat. *J. Am. Vet. Med. Assoc.* **200**:521–523.
11. **Shiota, T., M. Jones, M. Chikada, C. E. Fleishman, J. B. Castellucci, B. Cotter, A. N. DeMaria, O. T. von Ramm, J. Kisslo, T. Ryan, and D. J. Sahn.** 1998. Real-time three-dimensional echocardiography for determining right ventricular stroke volume in an animal model of chronic right ventricular volume overload. *Circulation.* **97**(10):1897–1900.
12. **Ratcliffe, M. B., A. W. Wallace, A. Salahieh, J. Hong, S. Ruch, and T. S. Hall.** 2000. Ventricular volume, chamber stiffness, and function after anteroapical aneurysm plication in sheep. *J. Thorac. Cardiovasc. Surg.* **119**(1):115–124.
13. **Thomas, W. P., C. E. Gaber, G. J. Jacobs, et al.** 1993. Recommendations for standards in transthoracic two-dimensional echocardiography in the dog and cat. Echocardiography Committee of the Specialty of Cardiology, American College of Veterinary Internal Medicine. *J. Vet. Intern. Med.* **7**:247–252.
14. **Kirberger, R. M., and J. S. van den Berg.** 1993. Pulsed wave Doppler echocardiographic evaluation of intracardiac blood flow in normal sheep. *Res. Vet. Sci.* **55**(2):189–194, 1992.
15. **Power, J. M., G. A. Beacom, C. A. Alferness, J. Raman, S. J. Farish, and A. M. Tonkin.** 1998. Effects of left atrial dilatation on the endocardial atrial defibrillation threshold: a study in an ovine model of pacing induced dilated cardiomyopathy. *Pacing Clin. Electrophysiol.* **21**(8):1595–1600
16. **Schmidt, K. G., N. H. Sliverman, and A. M. Rudolph.** 1998. Phasic flow events at the aortic isthmus-ductus arteriosus junction and branch pulmonary artery evaluated by multimodal ultrasonography in fetal lambs. *Am. J. Obstetr. Gynecol.* **179**(5):1338–1347.
17. **Ziekiewicz, M., B. Perek, B. Meyns, L. Mesotten, G. Dispersyn, Y. Nishimura, and W. Flameng.** 1999. Chronic heart failure model induced by coronary embolism in sheep. *Int. J. Artificial Organs.* **22**(7):499–504.
18. **Van Nooten, G., S. Ozaki, P. Herijgers, Y. Van Belegem, and W. Flameng.** 1999. Deformation of the stentless porcine valve scaffold enhances accelerated leaflet fibrosis and calcification in juvenile sheep. *Semin. Thorac. Cardiovasc. Surg.* **11**(4 Suppl 1):163–170.
19. **Solowiejczyk, D. E., I. Yamada, E. G. Cape, R. A. Manduley, W. M. Gersony, M. Jones, and L. M. Valdes-Cruz.** 1998. Simultaneous Doppler and catheter transvalvular pressure gradients across St. Jude bileaflet mitral valve prosthesis: in vivo study in a chronic animal model with pediatric valve sizes. *J. Am. Soc. Echocardiogr.* **11**(2):1145–1154.
20. **Palma, A., D. A. Hoffman, M. Nanna, S. Fernandes, and D. A. Sisto.** 1991. Transesophageal echocardiography for the evaluation of mitral valve prostheses in the weanling sheep. *ASAIO Trans.* **37**:M169–170.
21. **Kunzelman, K. S., D. T. Linker, S. Sai, C. Miyake-Hull, D. Quick, R. Thomas, G. Rothnie, and R. P. Cohran.** 1999. Acute mitral valve regurgitation created in sheep using echocardiographic guidance. *J. Heart Valve Dis.* **8**(6):637–643.